

Article

# Cd<sup>2+</sup>-Selective Fluorescence Enhancement of Bisquinoline Derivatives with 2-Aminoethanol Skeleton

Yuji Mikata <sup>1,2,3,4,\*</sup> , Aya Tsuruta <sup>3</sup>, Hinata Koike <sup>4</sup>, Sunao Shoji <sup>1,4</sup>  and Hideo Konno <sup>5</sup> 

<sup>1</sup> Laboratory for Molecular & Functional Design, Department of Engineering, Nara Women's University, Nara 630-8506, Japan

<sup>2</sup> KYOUSEI Science Center, Nara Women's University, Nara 630-8506, Japan

<sup>3</sup> Department of Chemistry, Biology and Environmental Science, Faculty of Science, Nara Women's University, Nara 630-8506, Japan

<sup>4</sup> Cooperative Major in Human Centered Engineering, Nara Women's University, Nara 630-8506, Japan

<sup>5</sup> National Institute of Advanced Industrial Science and Technology (AIST), 1-1-1 Higashi, Tsukuba 305-8565, Japan

\* Correspondence: mikata@cc.nara-wu.ac.jp

**Abstract:** The development of fluorescent Cd<sup>2+</sup> sensors requires strict selectivity over Zn<sup>2+</sup> because of the high availability of Zn<sup>2+</sup> in the natural environment. In this paper, bisquinoline-based fluorescent sensors with a 2-aminoethanol backbone were investigated. The weak coordination ability of quinoline compared to well-studied pyridine is suitable for Cd<sup>2+</sup> selectivity rather than Zn<sup>2+</sup>. In the presence of 3 equiv. of metal ions, TriMeO-*N,O*-BQMAE (*N,O*-bis(5,6,7-trimethoxy-2-quinolylmethyl)-2-methylaminoethanol (3)), as well as its *N,N*-isomer TriMeO-*N,N*-BQMAE (*N,N*-bis(5,6,7-trimethoxy-2-quinolylmethyl)-2-methoxyethylamine (6)), exhibits Cd<sup>2+</sup>-selective fluorescence enhancement over Zn<sup>2+</sup> in DMF-HEPES buffer (1:1, 50 mM HEPES, 0.1 M KCl, pH = 7.5) ( $I_{Zn}/I_{Cd} = 26\text{--}34\%$ ), which has similar selectivity in comparison to the corresponding ethylenediamine derivative TriMeOBQDMEN (*N,N'*-bis(5,6,7-trimethoxy-2-quinolylmethyl)-*N,N'*-dimethylethylenediamine) under the same experimental condition ( $I_{Zn}/I_{Cd} = 24\%$ ). The fluorescence mechanisms of *N,O*- and *N,N*-isomers of BQMAE are quite different, judging from the fluorescence lifetimes of their metal complexes. The Cd<sup>2+</sup> complex with TriMeO-*N,O*-BQMAE (3) exhibits a long fluorescence lifetime similar to that of TriMeOBQDMEN via intramolecular excimer emission, whereas the Cd<sup>2+</sup> complex with TriMeO-*N,N*-BQMAE (6) exhibits a short lifetime from monomer emission.

**Keywords:** cadmium; fluorescence; sensor; zinc; quinoline; 2-aminoethanol; ligand effect



**Citation:** Mikata, Y.; Tsuruta, A.; Koike, H.; Shoji, S.; Konno, H. Cd<sup>2+</sup>-Selective Fluorescence Enhancement of Bisquinoline Derivatives with 2-Aminoethanol Skeleton. *Molecules* **2024**, *29*, 369. <https://doi.org/10.3390/molecules29020369>

Academic Editors: Anna Cleta Croce, Andrea Bencini and Vito Lippolis

Received: 30 November 2023

Revised: 7 January 2024

Accepted: 8 January 2024

Published: 11 January 2024



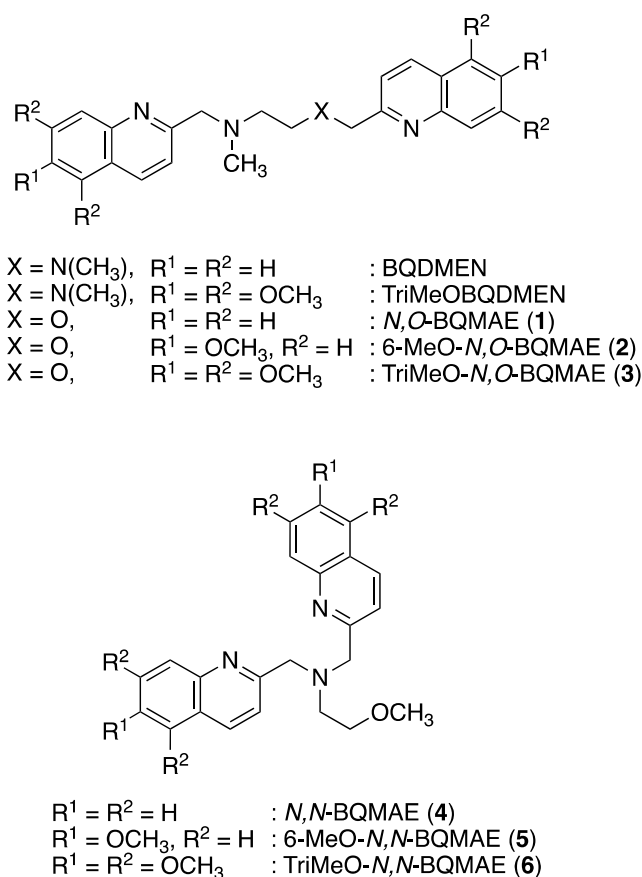
**Copyright:** © 2024 by the authors. Licensee MDPI, Basel, Switzerland. This article is an open access article distributed under the terms and conditions of the Creative Commons Attribution (CC BY) license (<https://creativecommons.org/licenses/by/4.0/>).

## 1. Introduction

Cadmium is a toxic metal and exists in vast areas of natural environments. Extensive use of cadmium in industry, including batteries and pigments, facilitates the exposure of cadmium to the air, water, and soils. As a result, cadmium-related health problems in humans are recent serious concerns [1,2]. In this context, the detection and quantification of cadmium in the environment, especially in water, are of urgent demand [3–5].

The fluorescence method is a powerful tool for the detection of metal ions and biologically important small molecules [6–15]. Its sensitivity, rapidness, and convenience allow us to visualize the target effectively. Specificity is the most important requisite for fluorescence sensing and owes to the rational molecular design of fluorescent probes. One of the most difficult and important problems in fluorescence detection is the discrimination between Cd<sup>2+</sup> and Zn<sup>2+</sup> because these two metal ions slightly differ in their ionic radii, which is only 21 pm [16–19]. The weak basicity of the quinoline nitrogen atom compared to that of pyridine offers a suitable coordination environment around the larger and softer Cd<sup>2+</sup> center than Zn<sup>2+</sup>. Therefore, many quinoline-based fluorescent Cd<sup>2+</sup> sensors have been extensively developed [20–25].

In our laboratory, several fluorescent probes for  $Zn^{2+}$  and  $Cd^{2+}$  based on the polyquinoline structure have been reported [26]. Considering the larger coordination number of  $Cd^{2+}$  in comparison to  $Zn^{2+}$ , the hepta- and octadentate tetrakisquinoline derivatives such as TQOPEN [27] (*N,N,N',N'*-tetrakis(2-quinolylmethyl)-3-oxa-1,5-pentanediamine) and TriMeOBAPTQ [28] (*N,N,N',N'*-tetrakis(5,6,7-trimethoxy-2-quinolylmethyl)-2,2'-(*N,N'*-dimethylethylenediamine)dianiline) were developed. Recently, the tetradentate bisquinoline derivative TriMeOBQDMEN [29] (*N,N'*-bis(5,6,7-trimethoxy-2-quinolylmethyl)-*N,N'*-dimethylethylenediamine, Scheme 1) opened the door to a new field of easily accessible small molecular fluorescent sensors for  $Cd^{2+}$ . The TriMeOBQDMEN exhibits  $Cd^{2+}$ -selective fluorescence enhancement in DMF- $H_2O$  (1:1) ( $I_{Zn}/I_{Cd} = 22\%$  in the presence of 1 equiv. of metal ion). The fluorescent  $Cd^{2+}/Zn^{2+}$  discrimination mechanism of TriMeOBQDMEN is not fully understood; however, the bis( $\mu$ -chloro) dicadmium complex was characterized using BQDMEN (Scheme 1) as a plausible fluorescent species [29]. In order to further develop the potential of tetradentate bisquinoline derivatives as  $Cd^{2+}$ -specific fluorescent sensors, here we designed oxygen-containing N3O1 tetradentate bisquinoline derivatives of BQDMEN, namely, *N,O*-BQMAE (*N,O*-bis(2-quinolylmethyl)-2-methylaminoethanol (1)) and its methoxy-substituted analogs 2 and 3 (Scheme 1). These oxygen-containing ligands were expected to possess reduced metal binding affinity compared with N4 tetradentate ligands and, therefore, a library with a set of fluorescent ligands with a wide variety of thresholds to quantify the concentration of  $Cd^{2+}$  can be constructed. Moreover, *N,N*-BQMAE (*N,N*-bis(2-quinolylmethyl)-2-methoxyethylamine (4)) and its methoxy-substituted analogs 5 and 6 (Scheme 1) were also examined as a set of regioisomers of *N,O*-BQMAE derivatives to expand the compound library.



**Scheme 1.** Structure of ligands.

## 2. Results and Discussion

### 2.1. Synthesis of Ligands

The newly designed six ligands (1–6) based on a 2-aminoethanol skeleton were prepared according to Scheme S1 using corresponding amines and methoxy-substituted chloromethylquinolines. N-alkylation of 2-methylaminoethanol followed by O-alkylation using *n*-butyllithium affords 1–3 in quite low yields (6–19%) due to the unoptimized experimental procedure for the second step. The synthesis of 4–6 was conducted in one step, starting from 2-methoxyethylamine in excellent yields (96% to quantitative yield). Structure and purity of ligands 3–6 were supported by  $^1\text{H}/^{13}\text{C}$  NMR and elemental analysis. Structure of ligands 1 and 2 was confirmed by  $^1\text{H}/^{13}\text{C}$  NMR. The complicated coupling pattern at the aliphatic proton region of 2 in  $^1\text{H}$  NMR spectrum is still under investigation.

### 2.2. Fluorescence Spectral Changes of *N,O*-BQMAE Derivatives 1–3

The metal ion-induced fluorescence spectral changes of *N,O*-BQMAE derivatives 1–3 were examined in DMF-HEPES buffer (1:1, 50 mM HEPES, 0.1 M KCl, pH = 7.5) (Figure 1a–f). Absorbance spectral changes and excitation spectrum for 3 are shown in Figure S1. The previously reported N4 tetradentate fluorescent  $\text{Cd}^{2+}$  sensor TriMeOBQDMEN [29] was also re-examined in DMF-HEPES buffer (1:1, 50 mM HEPES, 0.1 M KCl, pH = 7.5) in this study for strict comparison (Figure 1g,h) because all measurements in the previous report for TriMeOBQDMEN were performed in DMF- $\text{H}_2\text{O}$  solution. As shown in Figure 1, only trimethoxy-substituted derivative 3 from the *N,O*-BQMAE derivatives exhibits distinct fluorescence enhancement upon addition of metal ions. The *N,O*-BQMAE (1) bearing unsubstituted quinolines does not respond to any metal ions except for a small response toward  $\text{Cd}^{2+}$ ,  $\text{Zn}^{2+}$ , and  $\text{Pb}^{2+}$  (Figure 1b). The mono-methoxy derivative 6-MeO-*N,O*-BQMAE (2) only exhibits a  $\text{Cu}^{2+}$ -induced fluorescence quenching (Figure 1d). The trimethoxy derivative TriMeO-*N,O*-BQMAE (3) affords apparent  $\text{Cd}^{2+}$ -selective fluorescence enhancement over  $\text{Zn}^{2+}$  ( $I_{\text{Zn}}/I_{\text{Cd}} = 34\%$ ) (Figure 1f), which is a bit diminished in selectivity in comparison with TriMeOBQDMEN under the same experimental condition ( $I_{\text{Zn}}/I_{\text{Cd}} = 24\%$ ) (Figure 1h and Table 1).

The metal binding affinity ( $K_d$ ) was calculated from the non-linear fitting of titration curves with  $\text{Cd}^{2+}$  and  $\text{Zn}^{2+}$ , indicating that TriMeO-*N,O*-BQMAE (3) has two orders lower metal binding ability than TriMeOBQDMEN (Figures S3 and S4 and Table 1). This is because the coordination ability of the nitrogen atom is higher than that of oxygen, but two orders of difference are quite significant for such a small modification.

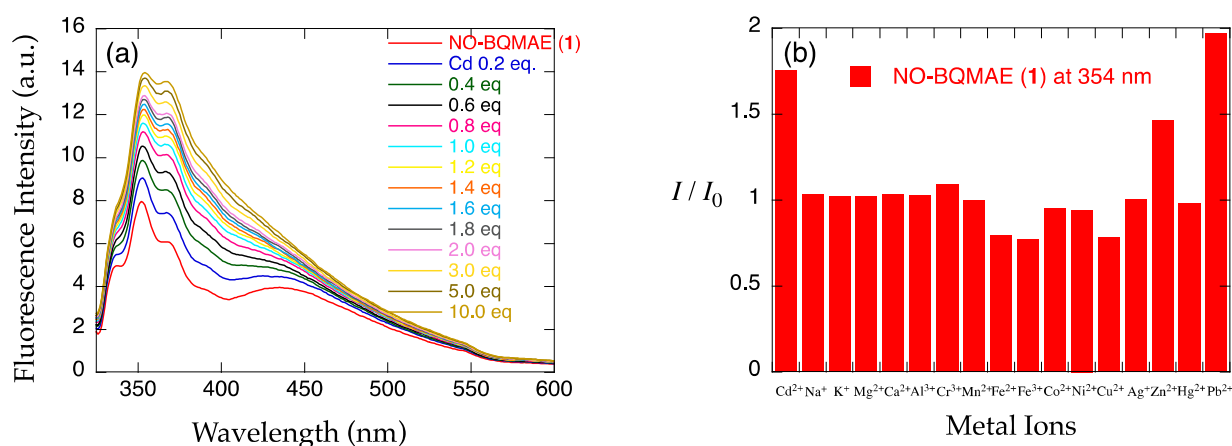
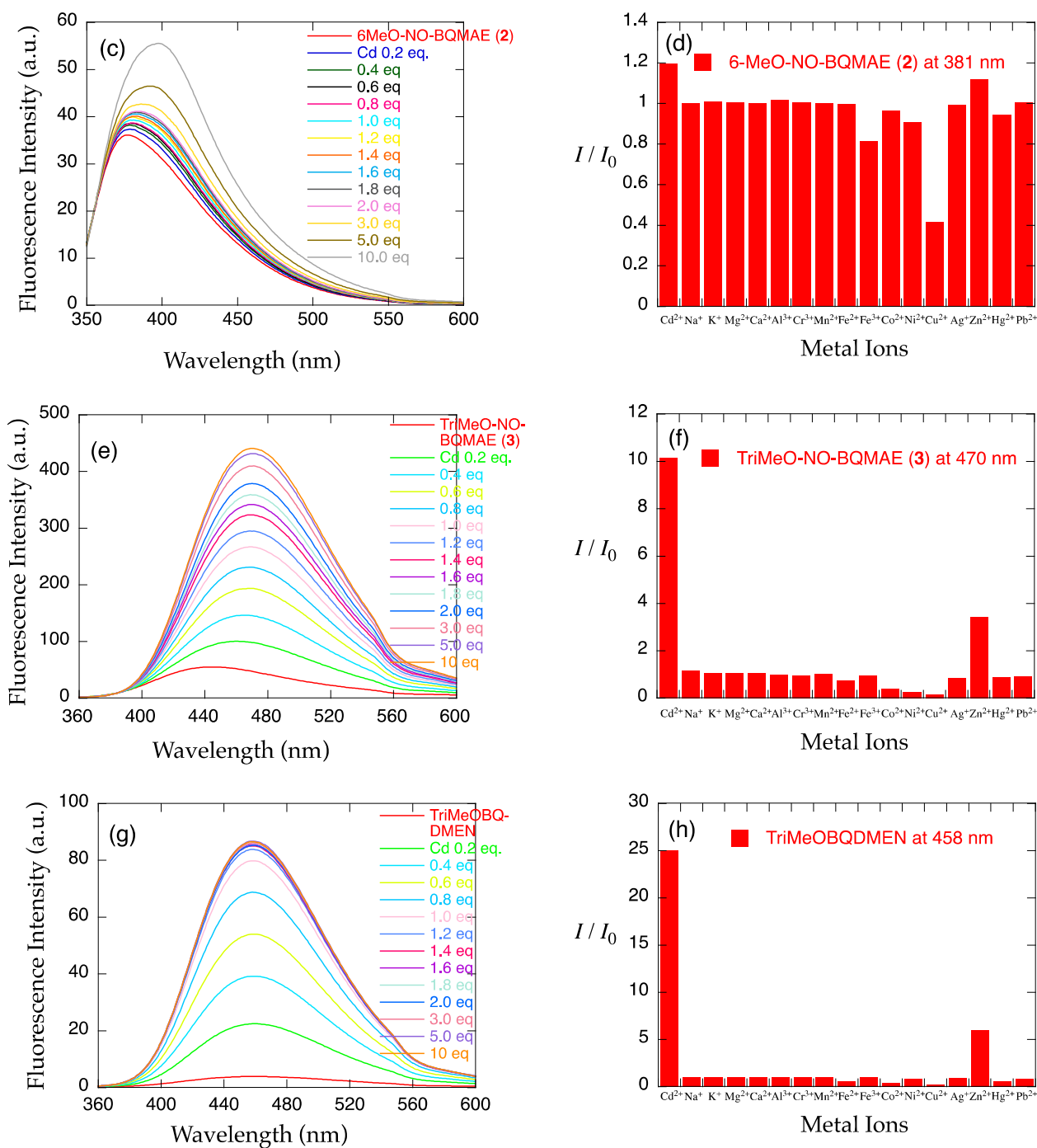


Figure 1. Cont.



**Figure 1.** (a,c,e,g) Fluorescence spectral changes and (b,d,f,h) relative fluorescence intensity of 34  $\mu\text{M}$  (a,b) *N,O*-BQMAE (1) ( $\lambda_{\text{ex}} = 317 \text{ nm}$ ), (c,d) 6-MeO-*N,O*-BQMAE (2) ( $\lambda_{\text{ex}} = 336 \text{ nm}$ ), (e,f) TriMeO-*N,O*-BQMAE (3) ( $\lambda_{\text{ex}} = 338 \text{ nm}$ ), and (g,h) TriMeOBQDMEN ( $\lambda_{\text{ex}} = 335 \text{ nm}$ ) in DMF-HEPES buffer (1:1, 50 mM HEPES, 0.1 M KCl, pH = 7.5) at 25 °C (a,c,e,g) in the presence of increasing concentrations of Cd<sup>2+</sup> and (b,d,f,h) in the presence of 3 equiv. of metal ions.  $I_0$  is the emission intensity of free ligand.

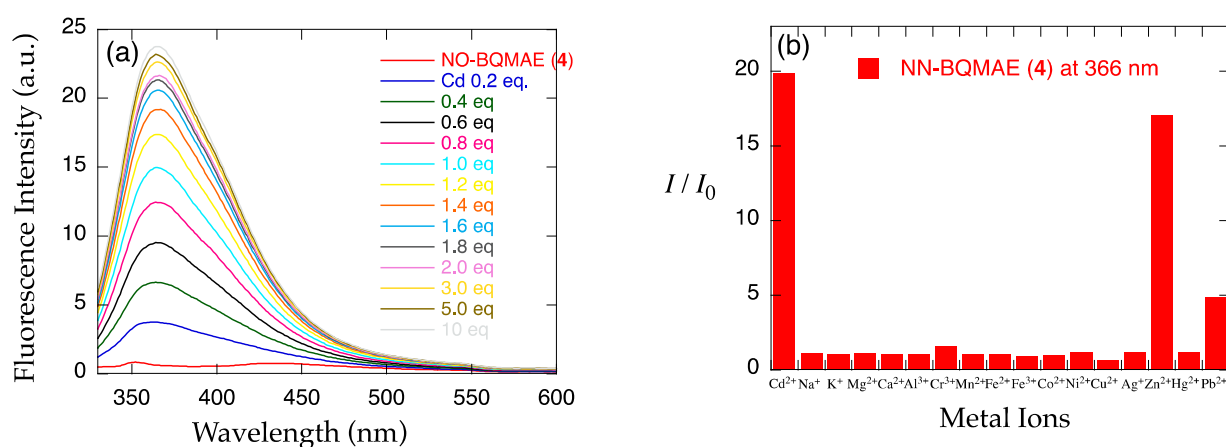
**Table 1.** Fluorescent and Thermodynamic Properties for Cd<sup>2+</sup> and Zn<sup>2+</sup> Complexes of BQMAE Derivatives 3–6 and TriMeOBQDMEN <sup>a</sup>.

Ligand	$\lambda_{ex}$ (nm)	$\lambda_{em}$ (nm) <sup>b</sup>	$I_{Zn}/I_{Cd}$ <sup>c</sup>	$\Phi_{Cd}$	$K_d$ for Cd <sup>2+</sup> Complex (M)	$K_d$ for Zn <sup>2+</sup> Complex (M)
TriMeO- <i>N,O</i> -BQMAE (3)	338	470	34%	0.281 <sup>d</sup>	$(1.4 \pm 0.2) \times 10^{-5}$	$(8.2 \pm 0.4) \times 10^{-5}$
<i>N,N</i> -BQMAE (4)	317	366	87%	0.018 <sup>d</sup>	$(8.1 \pm 1.5) \times 10^{-6}$	$(5.2 \pm 0.3) \times 10^{-5}$
6-MeO- <i>N,N</i> -BQMAE (5)	337	404	51%	0.171 <sup>d</sup>	$(6.4 \pm 0.3) \times 10^{-7}$	$(1.6 \pm 0.2) \times 10^{-5}$
TriMeO- <i>N,N</i> -BQMAE (6)	340	465	26%	0.228 <sup>d</sup>	$\sim 10^{-7}$	$(1.5 \pm 0.2) \times 10^{-5}$
TriMeOBQDMEN	335	458	24% (41% <sup>e</sup> )	0.293 <sup>c,e</sup>	$(2.6 \pm 1.0) \times 10^{-7}$	$(2.7 \pm 0.5) \times 10^{-6}$

<sup>a</sup> In DMF-HEPES buffer (1:1, 50 mM HEPES, 0.1 M KCl, pH = 7.5) at 25 °C. <sup>b</sup> For Cd<sup>2+</sup> complex. <sup>c</sup> In the presence of 3 equiv. of metal ions. <sup>d</sup> In the presence of 10 equiv. of metal ions. <sup>e</sup> In DMF-H<sub>2</sub>O (1:1) [29].

### 2.3. Fluorescence Spectral Changes of *N,N*-BQMAE Derivatives 4–6

The metal ion-induced fluorescence spectral changes of *N,N*-BQMAE derivatives 4–6 were next examined (Figure 2). Absorbance spectral changes and excitation spectrum for 6 are shown in Figure S2. Because of the synthetic inconvenience of *N,O*-BQMAE derivatives 1–3 and disappointing fluorescence response of 1 and 2 toward metal ions due to the weak metal binding ability of these compounds, the other N3O1 ligands with a bis(2-quinolylmethyl)amine moiety were explored. As shown in Figure 2, even in the unsubstituted quinoline derivative *N,N*-BQMAE (4), metal-induced fluorescence enhancement was clearly observed, which is largely different from the *N,O*-isomer 1 and 2. In the presence of a large excess of metal ions to assure the complete complexation, Zn<sup>2+</sup> induces a slightly higher fluorescence intensity of 4 than Cd<sup>2+</sup> (Figure S5). Other methoxy-substituted derivatives, including TriMeO-*N,O*-BQMAE (3) and TriMeOBQDMEN in the previous section, show complete metal binding in the presence of 3 equiv. of metal ions, and exhibit consistent preference of Cd<sup>2+</sup> over Zn<sup>2+</sup> (Figures S3, S4, S6 and S7). As the number of methoxy substituents increases, the fluorescence Cd<sup>2+</sup> selectivity is improved (Figure 2b,d,f, and Table 1), and the metal binding affinity is enhanced (Figures S5–S7 and Table 1). The three trimethoxy-substituted derivatives, namely, TriMeO-*N,O*-BQMAE (3) ( $K_{d(Zn)} = \sim 10^{-4}$ ), TriMeO-*N,N*-BQMAE (6) ( $K_{d(Zn)} = \sim 10^{-5}$ ), and TriMeOBQDMEN ( $K_{d(Zn)} = \sim 10^{-6}$ ) exhibit approximately one order different metal binding affinities in this order (Table 1). Since the fluorescence metal ion selectivity of these compounds is essentially the same ( $I_{Zn}/I_{Cd} = \sim 30\%$ ), this ligand library is a nice set of fluorescent sensors with different metal binding affinities, which is useful for convenient determination of Cd<sup>2+</sup> concentration.

**Figure 2.** Cont.

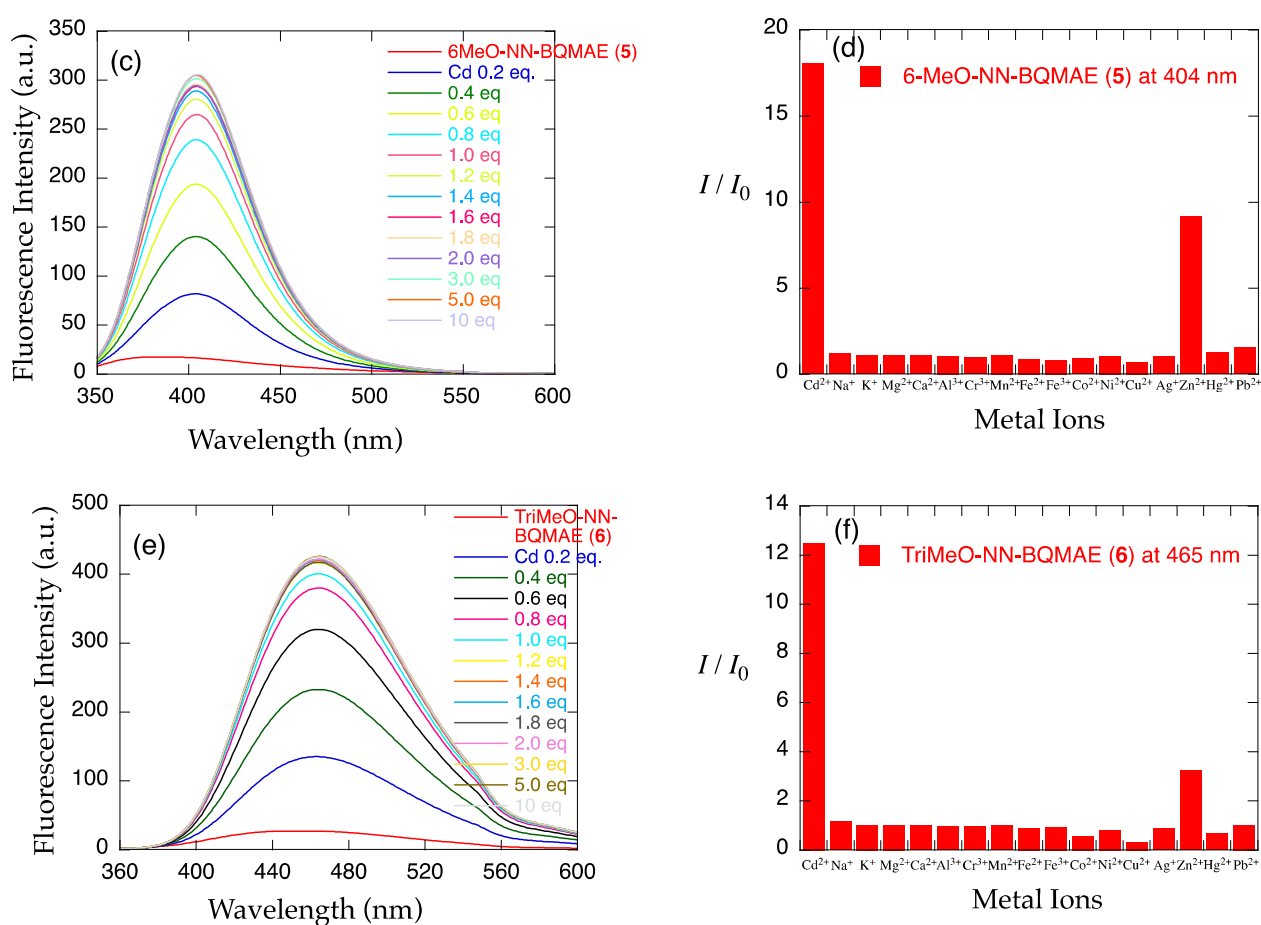


**Figure 2.** (a,c,e) Fluorescence spectral changes and (b,d,f) relative fluorescence intensity of 34  $\mu\text{M}$  (a,b) *N,N*-BQMAE (4) ( $\lambda_{\text{ex}} = 317 \text{ nm}$ ), (c,d) 6-MeO-*N,N*-BQMAE (5) ( $\lambda_{\text{ex}} = 337 \text{ nm}$ ), and (e,f) TriMeO-*N,N*-BQMAE (6) ( $\lambda_{\text{ex}} = 340 \text{ nm}$ ) in DMF-HEPES buffer (1:1, 50 mM HEPES, 0.1 M KCl, pH = 7.5) at 25 °C (a,c,e) in the presence of increasing concentrations of  $\text{Cd}^{2+}$  and (b,d,f) in the presence of 3 equiv. of metal ions.  $I_0$  is the emission intensity of free ligand.

#### 2.4. Effect of pH and Estimation of LOD

The effect of pH on the fluorescence intensity of the  $\text{Cd}^{2+}$  complex with TriMeO-*N,O*-BQMAE (3) and TriMeO-*N,N*-BQMAE (6) was examined (Figure 3). Protonation to the ligand at low pH region and coordination of hydroxide ion to  $\text{Cd}^{2+}$  at high pH region prevent the binding of  $\text{Cd}^{2+}$  to the probes. The pH window for fluorescent detection of  $\text{Cd}^{2+}$  is wider for 6 (Figure 3b) than 3 (Figure 3a), reflecting the difference in metal binding affinity of the ligands (Table 1). For 6, fluorescence intensity is fairly stable between pH = 4 and pH = 11. The limit of detection (LOD) for 6 was estimated as low as 17 nM (Figure S8), which is comparable to the other tetradentate fluorescent  $\text{Cd}^{2+}$  probes in the literature [24,30,31]. This value (LOD = 17 nM) is lower than the environmental limit of water in Japan (3 ppb, 27 nM). Accordingly, the limit of quantitation (LOQ) is calculated to be 57 nM. The above properties of TriMeO-*N,N*-BQMAE (6) demonstrate the potential of this ligand for practical uses.

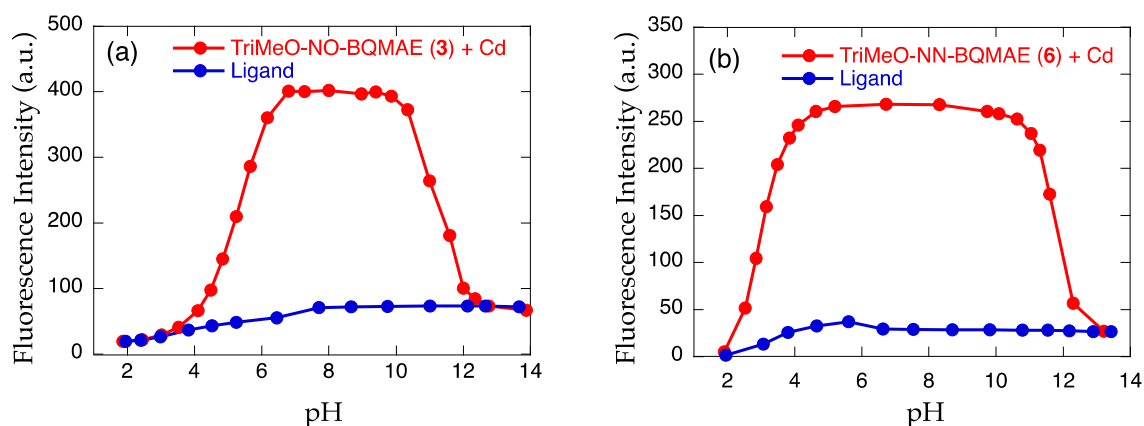


**Figure 3.** Effect of pH on the fluorescence intensity of (a) TriMeO-*N,O*-BQMAE (3) and (b) TriMeO-*N,N*-BQMAE (6) in the absence (blue) and presence (red) of 3 equiv. of  $\text{Cd}^{2+}$  in DMF-HEPES buffer (1:1, 50 mM HEPES, 0.1 M KCl, pH = 7.5) at 25 °C.

### 2.5. Fluorescence Lifetimes of *N,O*- and *N,N*-BQMAE Derivatives 3–6 and TriMeOBQDMEN

The fluorescence lifetimes ( $\tau$ ) for  $\text{Cd}^{2+}$  and  $\text{Zn}^{2+}$  complexes with *N,O*- and *N,N*-BQMAE derivatives 3–6 were measured in the presence of 2 equiv. of metal ions, in which most of the ligands form metal complexes. For comparison, TriMeOBQDMEN was also re-examined in DMF-HEPES buffer (1:1, 50 mM HEPES, 0.1 M KCl, pH = 7.5). Table 2 summarizes the results.

**Table 2.** Fluorescence Lifetimes for  $\text{Cd}^{2+}$  and  $\text{Zn}^{2+}$  Complexes of BQMAE Derivatives 3–6 and TriMeOBQDMEN <sup>a,b</sup>.

Ligand	Metal Ion	$\lambda_{em}$ (nm)	BPF (nm) <sup>c</sup>	$\tau$ (nsec) <sup>d</sup>
TriMeO- <i>N,O</i> -BQMAE (3)	—	—	460	1.2 (17%), 4.3 (74%), 14.5 (9%)
	$\text{Cd}^{2+}$	470	460	2.6 (5%), 11.5 (14%), 29.7 (81%)
	$\text{Zn}^{2+}$	484	460	2.1 (14%), 7.5 (34%), 22 (52%)
<i>N,N</i> -BQMAE (4)	—	—	370	1.2 (14%), 5.5 (40%)
	$\text{Cd}^{2+}$	364	370	5.4 (20%)
	$\text{Zn}^{2+}$	370	370	1.0 (43%), 5.3 (22%)
6-MeO- <i>N,N</i> -BQMAE (5)	—	—	400	2.7 (45%), 6.0 (46%)
	$\text{Cd}^{2+}$	404	400	1.1 (5%), 3.0 (1%), 6.2 (94%)
	$\text{Zn}^{2+}$	408	400	3.4 (27%), 6.8 (66%)
TriMeO- <i>N,N</i> -BQMAE (6)	—	—	460	1.2 (34%), 4.0 (24%), 16.8 (42%)
	$\text{Cd}^{2+}$	465	460	1.6 (2%), 8.5 (7%), 17.7 (91%)
	$\text{Zn}^{2+}$	480	490	1.2 (12%), 7.4 (33%), 16.5 (54%)
TriMeOBQDMEN	—	—	460	1.1 (29%), 4.3 (44%), 21.4 (27%)
	$\text{Cd}^{2+}$	472	460	3.5 (1%), 14.6 (5%), 31.8 (91%)
	$\text{Zn}^{2+}$	487	490	1.7 (2%), 7.8 (9%), 20.2 (88%)

<sup>a</sup> In DMF-HEPES buffer (1:1, 50 mM HEPES, 0.1 M KCl, pH = 7.5). <sup>b</sup> In the presence of 2 equiv. of metal ions. <sup>c</sup> Bandpass filter used ( $\pm 10$  nm). <sup>d</sup> Components with extremely short lifetimes (<1 nsec) were omitted.

As discussed previously for TriMeOBQDMEN based on the investigation in DMF- $\text{H}_2\text{O}$  solution [29], the fluorescent  $\text{Cd}^{2+}$  selectivity of this ligand is explained by the difference in fluorescence lifetime in  $\text{Cd}^{2+}$  and  $\text{Zn}^{2+}$  complexes, in which a very long ( $\tau = \sim 30$  nsec) lifetime was observed exclusively for the  $\text{Cd}^{2+}$  complex. From the crystal structure of the  $\text{Cd}^{2+}$  complex with BQDMEN ( $[\text{Cd}_2(\mu\text{-Cl})_2(\text{BQDMEN})_2]^{2+}$ ), this long lifetime was assigned to be an intramolecular excimer emission from the highly stacked two quinoline rings with interligand interaction. Interestingly, in DMF-HEPES buffer (1:1, 50 mM HEPES, 0.1 M KCl, pH = 7.5), this long fluorescence lifetime was preserved for the TriMeOBQDMEN- $\text{Cd}^{2+}$

complex ( $\tau = 32$  nsec) (Table 2). Here again, the  $\text{Zn}^{2+}$  complex with TriMeOBQDMEN exhibits a shorter lifetime ( $\tau = 20$  nsec) than  $\text{Cd}^{2+}$ . These results strongly support that the fluorescence lifetime is a critical measure for the mechanism of fluorescence and structure of the metal complexes, which is independent of the solvent system used for measurements.

Similar distinct difference in fluorescence lifetimes of  $\text{Cd}^{2+}$  and  $\text{Zn}^{2+}$  complexes was found for TriMeO-*N,O*-BQMAE (**3**) ( $\tau_{\text{Cd}} = 30$  nsec and  $\tau_{\text{Zn}} = 22$  nsec). This is because the ligand structure of *N,O*-BQMAE resembles that of BQDMEN (Scheme 1) and rationally suggests the specific formation of a bis( $\mu$ -chloro) dinuclear cadmium complex for **3**. On the other hand, the *N,N*-BQMAE derivatives did not exhibit any differences in fluorescence lifetimes between  $\text{Cd}^{2+}$  and  $\text{Zn}^{2+}$  complexes. Even in the trimethoxy-substituted TriMeO-*N,N*-BQMAE (**6**), the lifetimes for  $\text{Cd}^{2+}$  and  $\text{Zn}^{2+}$  complexes are completely the same ( $\tau_{\text{Cd}} = 18$  nsec and  $\tau_{\text{Zn}} = 17$  nsec), and these values are too short to consider the excimer formation discussed above. These values ( $\tau = \sim 20$  nsec) are in good agreement with those for monomer complexes such as TriMeOTQTACN [28] (*N,N',N''*-tris(5,6,7-trimethoxy-2-quinolylmethyl)-1,4,7-triazacyclononane) ( $\tau_{\text{Cd}} = 21$  nsec and  $\tau_{\text{Zn}} = 23$  nsec) measured in MeOH-HEPES buffer (1:1, 50 mM HEPES, 0.1 M KCl, pH = 7.5). As a result, TriMeO-*N,O*-BQMAE (**3**) and TriMeO-*N,N*-BQMAE (**6**) adopt a different fluorescence mechanism possibly due to the different complex structure. Slightly diminished fluorescence quantum yield of **6** ( $\phi_{\text{Cd}} = 0.23$ ) in comparison to those of **3** ( $\phi_{\text{Cd}} = 0.28$ ) and BQDMEN ( $\phi_{\text{Cd}} = 0.29$ ) (Table 1) may reflect such differences. Although extensive trials of crystallization of  $\text{Cd}^{2+}$  complexes of **1–6** have been unsuccessful so far, the proton NMR indicates the coordination of quinoline and methoxy moieties to the metal center for *N,N*-BQMAE (**4**)- $\text{Cd}^{2+}$  complex, affording the chemical shift changes (Figure S9). The characteristic peak splitting of the methylene signal around 4.4–4.7 ppm also supports the coordination of 2-aminomethylquinoline moiety to the metal center.

At the present stage, the details in the fluorescent  $\text{Cd}^{2+}/\text{Zn}^{2+}$  discrimination mechanism of TriMeO-*N,N*-BQMAE (**6**) is still unknown, but the dynamic equilibrium of mononuclear ( $[\text{Cd}(\text{L})\text{Cl}]^+$ ) and  $\mu$ -chloro-bridged dinuclear ( $[\text{Cd}_2(\mu\text{-Cl})_2(\text{L})_2]^{2+}$ ) cadmium complexes needs to be considered. To answer these critical questions, related projects using other ligand systems with different skeletons are now in progress in our laboratory.

### 3. Experimental

#### 3.1. Materials and Methods

All reagents and solvents used for the preparation of probe molecules were obtained from commercial sources and used as received. DMF (*N,N*-dimethylformamide) used for spectroscopic measurements was of spectral grade (Dojin, Spectrosol). All aqueous solutions were prepared using Milli-Q water (Millipore, Merck, Germany).  $^1\text{H}/^{13}\text{C}$  NMR spectra were recorded on a JEOL (Akishima, Japan) AL-400 (400/100 MHz) spectrometer and referenced to internal  $\text{Si}(\text{CH}_3)_4$  or solvent signal. Elemental analyses were recorded on J-Science (Kyoto, Japan) JM-10 micro corder. UV-vis and fluorescence spectra were measured on a Jasco (Hachioji, Japan) V-660 spectrophotometer and Jasco (Hachioji, Japan) FP-6300 spectrofluorometer, respectively. Fluorescence quantum yields were measured on a HAMAMATSU photonics (Hamamatsu, Japan) C9920-02 absolute PL quantum yield measurement system. Fluorescence lifetimes were measured on a HORIBA fluorescence lifetime system Temprow equipped with a 370, 400, 460, or 490 nm bandpath filter. TriMeOBQDMEN [29] was prepared as described previously. CAUTION: Perchlorate salts of metal complexes with organic ligands are potentially explosive. All due precautions should be taken.

#### 3.2. Synthesis of *N,O*-Bis(2-quinolylmethyl)-2-methylaminoethanol (*N,O*-BQMAE (**1**))

The mixture of 2-methylaminoethanol (37.6 mg, 0.501 mmol), 2-chloromethylquinoline (89.8 mg, 0.506 mmol), potassium carbonate (71.4 mg, 0.517 mmol), and potassium iodide (84.5 mg, 0.509 mmol) in dry acetonitrile (15 mL) was refluxed for 23 h. After the reaction mixture was cooled to room temperature, solvent was removed under reduced pressure,

and organic materials were extracted with dichloromethane–water. The organic layer was dried and evaporated to afford *N*-(2-quinolylmethyl)-2-methylaminoethanol as yellow oil (106 mg, 0.490 mmol, 98%).

This material (200 mg, 0.925 mmol) was dissolved in THF (4 mL) and cooled on ice, then *n*-butyllithium (1.6 M solution in hexane, 869  $\mu$ L, 1.39 mmol) was added slowly through a syringe. After stirring for 30 min on ice, 2-chloromethylquinoline (205 mg, 1.15 mmol) in THF (2 mL) was added slowly through a syringe. The reaction mixture was warmed to room temperature and refluxed for 2 h. After the reaction, solvent was removed under reduced pressure, and organic materials were extracted with dichloromethane–water. The organic layer was dried and evaporated, and the residue was purified by alumina column chromatography using chloroform containing 0.1% methanol ( $R_f = 0.25$ ) as an eluent. The product was further purified by recycling GPC to afford *N,O*-bis(2-quinolylmethyl)-2-methylaminoethanol (*N,O*-BQMAE (**1**)) as yellow oil (21.3 mg, 0.0596 mmol, 6%).

$^1\text{H}$  NMR ( $\text{CDCl}_3$ , 400 MHz):  $\delta$  (ppm) 8.03–8.15 (m, 4H, quinoline-H4 and H8), 7.78–7.82 (m, 2H, quinoline-H5), 7.67–7.72 (m, 3H, quinoline-H3 and H6), 7.62 (d,  $J = 8.3$  Hz, 1H, quinoline-H3), 7.49–7.54 (m, 2H, quinoline-H7), 4.84 (s, 2H,  $\text{OCH}_2\text{Ar}$ ), 3.94 (s, 2H,  $\text{NCH}_2\text{Ar}$ ), 3.77 (t,  $J = 5.6$  Hz, 2H,  $\text{OCH}_2\text{CH}_2$ ), 2.85 (t,  $J = 5.6$  Hz, 2H,  $\text{NCH}_2\text{CH}_2$ ), 2.41 (s, 3H,  $\text{NCH}_3$ ).

$^{13}\text{C}$  NMR ( $\text{CDCl}_3$ , 100 MHz):  $\delta$  (ppm) 160.2, 259.3, 147.6, 147.5, 136.7, 136.3, 129.5, 129.3, 129.0, 128.9, 127.6, 127.5, 126.2, 126.1, 121.1, 119.3, 74.6, 69.1, 64.8, 57.0, 43.3.

HRMS (ESI)  $m/z$ : [**1** + Na] $^+$  calcd. for  $\text{C}_{23}\text{H}_{23}\text{N}_3\text{ONa}$  380.17388. Found 380.17026.

### 3.3. Synthesis of *N,O*-Bis(6-methoxy-2-quinolylmethyl)-2-methylaminoethanol (6-MeO-*N,O*-BQMAE (**2**))

The mixture of 2-methylaminoethanol (62.8 mg, 0.836 mmol), 6-methoxy-2-chloromethylquinoline (154 mg, 0.742 mmol), potassium carbonate (103 mg, 0.745 mmol), and potassium iodide (142 mg, 0.855 mmol) in dry acetonitrile (20 mL) was refluxed for 23 h. After the reaction mixture was cooled to room temperature, solvent was removed under reduced pressure, and organic materials were extracted with dichloromethane–water. The organic layer was dried and evaporated to afford *N*-(6-methoxy-2-quinolylmethyl)-2-methylaminoethanol as yellow oil in quantitative yield.

This material (183 mg, 0.742 mmol) was dissolved in THF (4 mL) and cooled on ice, then *n*-butyllithium (1.6 M solution in hexane, 798  $\mu$ L, 1.28 mmol) was added slowly through a syringe. After stirring for 30 min on ice, 6-methoxy-2-chloromethylquinoline (177 mg, 0.852 mmol) in THF (2 mL) was added slowly through a syringe. The reaction mixture was warmed to room temperature and refluxed for 2 h. After the reaction, solvent was removed under reduced pressure, and organic materials were extracted with dichloromethane–water. The organic layer was dried and evaporated, and the residue was purified by alumina column chromatography using chloroform containing 0.3% methanol ( $R_f = 0.3$ ) as an eluent. The product was further purified by recycling GPC to afford *N,O*-bis(6-methoxy-2-quinolylmethyl)-2-methylaminoethanol (6-MeO-*N,O*-BQMAE (**2**)) as brown oil (54.8 mg, 0.131 mmol, 18%).

$^1\text{H}$  NMR ( $\text{CDCl}_3$ , 400 MHz):  $\delta$  (ppm) 7.95–8.00 (m, 3H, quinoline-H4 and H8), 7.89 (d,  $J = 8.3$  Hz, 1H, quinoline-H8), 7.29–7.37 (m, 4H, quinoline-H3 and H7), 7.04 (d,  $J = 2.9$  Hz, 1H, quinoline-H5), 7.01 (d,  $J = 2.9$  Hz, 1H, quinoline-H5), 4.68 (t,  $J = 7.3$  Hz, 1H,  $\text{OCH}_2\text{Ar}$ ), 4.0–4.5 (br., 1H,  $\text{OCH}_2\text{Ar}$ ), 3.92 (s, 3H,  $\text{OCH}_3$ ), 3.90 (s, 3H,  $\text{OCH}_3$ ), 3.56–3.76 (m, 4H,  $\text{NCH}_2\text{Ar}$  and  $\text{OCH}_2\text{CH}_2$ ), 2.91–2.98 (m, 1H,  $\text{NCH}_2\text{CH}_2$ ), 2.61–2.65 (m, 1H,  $\text{NCH}_2\text{CH}_2$ ), 2.36 (s, 3H,  $\text{NCH}_3$ ).

$^{13}\text{C}$  NMR ( $\text{CDCl}_3$ , 100 MHz):  $\delta$  (ppm) 158.1, 157.6, 157.3, 157.0, 143.8, 143.5, 134.9, 134.6, 130.8, 130.1, 128.1, 127.6, 122.8, 122.0, 121.9, 105.1, 105.1, 68.6, 58.7, 55.53, 55.48, 55.42, 38.5, 38.1.

HRMS (ESI)  $m/z$ : [**2** + H] $^+$  calcd. for  $\text{C}_{25}\text{H}_{28}\text{N}_3\text{O}_3$  418.21307. Found 418.22029.

### 3.4. Synthesis of *N,O*-Bis(5,6,7-trimethoxy-2-quinolylmethyl)-2-methylaminoethanol (TriMeO-*N,O*-BQMAE (3))

The mixture of 2-methylaminoethanol (59.0 mg, 0.786 mmol), 5,6,7-trimethoxy-2-chloromethylquinoline (199 mg, 0.743 mmol), potassium carbonate (105 mg, 0.760 mmol), and potassium iodide (125 mg, 0.753 mmol) in dry acetonitrile (20 mL) was refluxed for 23 h. After the reaction mixture was cooled to room temperature, solvent was removed under reduced pressure, and organic materials were extracted with dichloromethane–water. The organic layer was dried and evaporated to afford *N*-(5,6,7-trimethoxy-2-quinolylmethyl)-2-methylaminoethanol as yellow oil in quantitative yield.

This material (220 mg, 0.718 mmol) was dissolved in THF (4 mL) and cooled on ice, then *n*-butyllithium (1.6 M solution in hexane, 675  $\mu$ L, 1.08 mmol) was added slowly through a syringe. After stirring for 30 min on ice, 5,6,7-trimethoxy-2-chloromethylquinoline (195 mg, 0.728 mmol) in THF (2 mL) was added slowly through a syringe. The reaction mixture was warmed to room temperature and refluxed for 2 h. After the reaction, solvent was removed under reduced pressure, and organic materials were extracted with dichloromethane–water. The organic layer was dried and evaporated, and the residue was purified by alumina column chromatography using chloroform containing 0.3% methanol ( $R_f = 0.4$ ) as an eluent. The product was further purified by recycling GPC to afford *N,O*-bis(5,6,7-trimethoxy-2-quinolylmethyl)-2-methylaminoethanol (TriMeO-*N,O*-BQMAE (3)) as brown oil (73.2 mg, 0.136 mmol, 19%).

$^1\text{H}$  NMR ( $\text{CDCl}_3$ , 400 MHz):  $\delta$  (ppm) 8.34 (d,  $J = 8.8$  Hz, 1H, quinoline-H4), 8.31 (d,  $J = 8.3$  Hz, 1H, quinoline-H4), 7.53 (d,  $J = 8.8$  Hz, 1H, quinoline-H3), 7.47 (d,  $J = 8.3$  Hz, 1H, quinoline-H3), 7.24 (s, 1H, quinoline-H8), 7.21 (s, 1H, quinoline-H8), 4.78 (s, 2H,  $\text{OCH}_2\text{Ar}$ ), 4.06 (s, 6H,  $\text{OCH}_3$ ), 4.00 (s, 6H,  $\text{OCH}_3$ ), 3.98 (s, 6H,  $\text{OCH}_3$ ), 3.89 (s, 2H,  $\text{NCH}_2\text{Ar}$ ), 3.77 (t,  $J = 5.6$  Hz, 2H,  $\text{OCH}_2\text{CH}_2$ ), 2.83 (t,  $J = 5.6$  Hz, 2H,  $\text{NCH}_2\text{CH}_2$ ), 2.40 (s, 3H,  $\text{NCH}_3$ ).

$^{13}\text{C}$  NMR ( $\text{CDCl}_3$ , 100 MHz):  $\delta$  (ppm) 158.4, 155.9, 155.7, 146.9, 145.3, 140.4, 130.9, 130.6, 118.8, 118.4, 118.1, 117.0, 103.9, 130.7, 74.5, 68.9, 64.7, 61.5, 61.2, 56.9, 56.0, 43.2.

Anal. Calcd for  $\text{C}_{29}\text{H}_{36.4}\text{N}_3\text{O}_{7.7}$  ( $3 \cdot 0.7\text{H}_2\text{O}$ ): H, 6.67; C, 63.31; N, 7.64. Found: H, 6.36; C, 63.16; N, 7.36.

HRMS (ESI)  $m/z$ :  $[\mathbf{3} + \text{H}]^+$  calcd. for  $\text{C}_{29}\text{H}_{36}\text{N}_3\text{O}_7$  538.25532. Found 538.25830.

### 3.5. Synthesis of *N,N*-Bis(2-quinolylmethyl)-2-methoxyethylamine (*N,N*-BQMAE (4))

The mixture of 2-methoxyethylamine (22.4 mg, 0.298 mmol), 2-chloromethylquinoline (88.6 mg, 0.499 mmol), and potassium carbonate (69.1 mg, 0.500 mmol) in dry acetonitrile (10 mL) was refluxed for 21 h. After the reaction mixture was cooled to room temperature, solvent was removed under reduced pressure, and organic materials were extracted with dichloromethane–water. The organic layer was dried and evaporated to afford *N,N*-bis(2-quinolylmethyl)-2-methoxyethylamine (*N,N*-BQMAE (4)) as a yellow-white solid in quantitative yield.

$^1\text{H}$  NMR ( $\text{CDCl}_3$ , 400 MHz):  $\delta$  (ppm) 8.13 (d,  $J = 8.7$  Hz, 2H, quinoline-H4), 8.04 (d,  $J = 8.3$  Hz, 2H, quinoline-H8), 7.76–7.81 (m, 4H, quinoline-H3 and H5), 7.68 (dt,  $J = 1.0$ , 8.3 Hz, 2H, quinoline-H6), 7.50 (t,  $J = 7.4$  Hz, 2H, quinoline-H7), 4.11 (s, 4H,  $\text{NCH}_2\text{Ar}$ ), 3.56 (t,  $J = 5.9$  Hz, 2H,  $\text{OCH}_2\text{CH}_2$ ), 3.27 (s, 3H,  $\text{OCH}_3$ ), 2.89 (t,  $J = 5.9$  Hz, 2H,  $\text{NCH}_2\text{CH}_2$ ).

$^{13}\text{C}$  NMR ( $\text{CDCl}_3$ , 100 MHz):  $\delta$  (ppm) 160.5, 147.5, 136.2, 129.3, 128.9, 127.4, 127.3, 126.0, 121.0, 71.0, 61.8, 58.6, 53.7.

Anal. Calcd for  $\text{C}_{23}\text{H}_{23.4}\text{N}_3\text{O}_{1.2}$  ( $4 \cdot 0.2\text{H}_2\text{O}$ ): H, 6.53; C, 76.51; N, 11.64. Found: H, 6.55; C, 76.56; N, 11.72.

HRMS (ESI)  $m/z$ :  $[\mathbf{4} + \text{Na}]^+$  calcd. for  $\text{C}_{23}\text{H}_{23}\text{N}_3\text{ONa}$  380.17388. Found 380.18173.

### 3.6. Synthesis of *N,N*-Bis(6-methoxy-2-quinolylmethyl)-2-methoxyethylamine (6-MeO-*N,N*-BQMAE (5))

The mixture of 2-methoxyethylamine (38.3 mg, 0.510 mmol), 6-methoxy-2-chloromethylquinoline (215 mg, 1.04 mmol), and potassium carbonate (138 mg, 0.998 mmol) in dry acetonitrile (20 mL) was refluxed for 21 h. After the reaction mixture was cooled to room

temperature, solvent was removed under reduced pressure, and organic materials were extracted with dichloromethane–water. The organic layer was dried and evaporated to afford *N,N*-bis(6-methoxy-2-quinolylmethyl)-2-methoxyethylamine (6-MeO-*N,N*-BQMAE (5)) as yellow oil (208 mg, 0.498 mmol, 96%).

$^1\text{H}$  NMR ( $\text{CDCl}_3$ , 400 MHz):  $\delta$  (ppm) 8.01 (d,  $J = 8.8$  Hz, 2H, quinoline-H4), 7.94 (d,  $J = 9.3$  Hz, 2H, quinoline-H8), 7.70 (d,  $J = 8.3$  Hz, 2H, quinoline-H3), 7.33 (dd,  $J = 2.9, 9.2$  Hz, 2H, quinoline-H7), 7.05 (d,  $J = 2.9$  Hz, 2H, quinoline-H5), 4.05 (s, 4H,  $\text{NCH}_2\text{Ar}$ ), 3.92 (s, 6H,  $\text{OCH}_3$ ), 3.55 (t,  $J = 5.6$  Hz, 2H,  $\text{OCH}_2\text{CH}_2$ ), 3.26 (s, 3H,  $\text{OCH}_3$ ), 2.87 (t,  $J = 5.6$  Hz, 2H,  $\text{NCH}_2\text{CH}_2$ ).

$^{13}\text{C}$  NMR ( $\text{CDCl}_3$ , 100 MHz):  $\delta$  (ppm) 157.8, 157.4, 134.4, 135.1, 130.3, 128.2, 121.8, 121.4, 105.1, 70.9, 61.5, 58.6, 55.4, 53.6.

Anal. Calcd for  $\text{C}_{25}\text{H}_{28}\text{N}_3\text{O}_{3.5}$  (5·0.5 $\text{H}_2\text{O}$ ): H, 6.62; C, 70.40; N, 9.85. Found: H, 6.42; C, 70.15; N, 9.80.

HRMS (ESI)  $m/z$ : [ $5 + \text{Na}$ ] $^+$  calcd. for  $\text{C}_{25}\text{H}_{27}\text{N}_3\text{O}_3\text{Na}$  440.19501. Found 440.20330.

### 3.7. Synthesis of *N,N*-Bis(5,6,7-trimethoxy-2-quinolylmethyl)-2-methoxyethylamine (TriMeO-*N,N*-BQMAE (6))

The mixture of 2-methoxyethylamine (27.3 mg, 0.363 mmol), 5,6,7-trimethoxy-2-chloromethylquinoline (201 mg, 0.751 mmol), and potassium carbonate (103 mg, 0.745 mmol) in dry acetonitrile (15 mL) was refluxed for 21 h. After the reaction mixture was cooled to room temperature, solvent was removed under reduced pressure, and organic materials were extracted with dichloromethane–water. The organic layer was dried and evaporated to afford *N,N*-bis(5,6,7-trimethoxy-2-quinolylmethyl)-2-methoxyethylamine (TriMeO-*N,N*-BQMAE (6)) as yellow oil in quantitative yield.

$^1\text{H}$  NMR ( $\text{CDCl}_3$ , 400 MHz):  $\delta$  (ppm) 8.31 (d,  $J = 8.3$  Hz, 2H, quinoline-H4), 7.62 (d,  $J = 8.8$  Hz, 2H, quinoline-H3), 7.20 (s, 2H, quinoline-H8), 4.04 (s, 10H,  $\text{NCH}_2\text{Ar}$  and  $\text{OCH}_3$ ), 3.98 (s, 6H,  $\text{OCH}_3$ ), 3.97 (s, 6H,  $\text{OCH}_3$ ), 3.57 (t,  $J = 5.6$  Hz, 2H,  $\text{OCH}_2\text{CH}_2$ ), 3.29 (s, 3H,  $\text{OCH}_3$ ), 2.87 (t,  $J = 5.6$  Hz, 2H,  $\text{NCH}_2\text{CH}_2$ ).

$^{13}\text{C}$  NMR ( $\text{CDCl}_3$ , 100 MHz):  $\delta$  (ppm) 159.9, 155.7, 146.9, 145.2, 140.4, 130.5, 118.7, 118.1, 103.9, 71.0, 61.7, 61.5, 61.1, 58.7, 56.0, 53.7.

Anal. Calcd for  $\text{C}_{29.3}\text{H}_{35.3}\text{Cl}_{0.9}\text{N}_3\text{O}_7$  (6·0.3 $\text{CHCl}_3$ ): H, 6.20; C, 61.37; N, 7.33. Found: H, 6.05; C, 61.66; N, 7.34.

HRMS (ESI)  $m/z$ : [ $6 + \text{Na}$ ] $^+$  calcd. for  $\text{C}_{29}\text{H}_{35}\text{N}_3\text{O}_7\text{Na}$  560.23727. Found 560.24627.

## 4. Conclusions

The newly designed six bisquinoline-based N3O1 tetradentate ligands with 2-aminoethanol backbone were examined as a fluorescent  $\text{Cd}^{2+}$  sensor. This ligand library includes *N,O*-BQMAE derivatives 1–3 and *N,N,O*-BQMAE derivatives 4–6, which differ in the position of two quinoline moieties and the number of methoxy substituents on the quinoline rings. Judging from the moderately good fluorescent  $\text{Cd}^{2+}$  selectivity over  $\text{Zn}^{2+}$  ( $I_{\text{Zn}}/I_{\text{Cd}} \sim 30\%$ ) and wide range of metal binding affinity (two orders differences in  $K_d$ ), the trimethoxy derivatives TriMeO-*N,O*-BQMAE (3) and TriMeO-*N,N*-BQMAE (6), as well as previously reported TriMeOBQDMEN, are regarded as a potential set of fluorescent ligands with different metal binding affinities useful for convenient quantification of  $\text{Cd}^{2+}$  in solution.

**Supplementary Materials:** The following supporting information can be downloaded at: <https://www.mdpi.com/article/10.3390/molecules29020369/s1>, Scheme S1: Synthesis of ligands 1–6; Figure S1: Absorbance spectral changes of 34  $\mu\text{M}$  *N,O*-BQMAE (1), 6-MeO-*N,O*-BQMAE (2), and TriMeO-*N,O*-BQMAE (3) in DMF-HEPES buffer (1:1, 50 mM HEPES, 0.1 M KCl, pH = 7.5) at 25 °C in the presence of increasing concentrations of  $\text{Cd}^{2+}$ ; Figure S2: Absorbance spectral changes of 34  $\mu\text{M}$  *N,N*-BQMAE (4), 6-MeO-*N,N*-BQMAE (5), and TriMeO-*N,N*-BQMAE (6) in DMF-HEPES buffer (1:1, 50 mM HEPES, 0.1 M KCl, pH = 7.5) at 25 °C in the presence of increasing concentrations of  $\text{Cd}^{2+}$ ; Figure S3: Estimation of dissociation constants ( $K_d$ ) for TriMeO-*N,O*-BQMAE (3) with  $\text{Cd}^{2+}$  and  $\text{Zn}^{2+}$  in DMF-HEPES buffer (1:1, 50 mM HEPES, 0.1 M KCl, pH = 7.5) at 25 °C; Figure S4: Estimation of dissociation constants ( $K_d$ ) for TriMeOBQDMEN with  $\text{Cd}^{2+}$  and  $\text{Zn}^{2+}$  in DMF-HEPES buffer (1:1,

50 mM HEPES, 0.1 M KCl, pH = 7.5) at 25 °C; Figure S5: Estimation of dissociation constants ( $K_d$ ) for *N,N*-BQMAE (4) with  $Cd^{2+}$  and  $Zn^{2+}$  in DMF-HEPES buffer (1:1, 50 mM HEPES, 0.1 M KCl, pH = 7.5) at 25 °C; Figure S6: Estimation of dissociation constants ( $K_d$ ) for 6-MeO-*N,N*-BQMAE (5) with  $Cd^{2+}$  and  $Zn^{2+}$  in DMF-HEPES buffer (1:1, 50 mM HEPES, 0.1 M KCl, pH = 7.5) at 25 °C; Figure S7: Estimation of dissociation constants ( $K_d$ ) for TriMeO-*N,N*-BQMAE (6) with  $Cd^{2+}$  and  $Zn^{2+}$  in DMF-HEPES buffer (1:1, 50 mM HEPES, 0.1 M KCl, pH = 7.5) at 25 °C; Figure S8: Estimation of LOD (limit of detection) for  $Cd^{2+}$  with TriMeO-*N,N*-BQMAE (6) in DMF-HEPES buffer (1:1, 50 mM HEPES, 0.1 M KCl, pH = 7.5) at 25 °C; Figure S9:  $^1H$  NMR spectrum of  $Cd^{2+}$  complex of *N,N*-BQMAE (4) in  $DMSO-d_6$ ; Figure S10:  $^1H/^{13}C$  NMR spectrum of *N,O*-BQMAE (1) in  $CDCl_3$ ; Figure S11:  $^1H/^{13}C$  NMR spectrum of 6-MeO-*N,O*-BQMAE (2) in  $CDCl_3$ ; Figure S12:  $^1H/^{13}C$  NMR spectrum of TriMeO-*N,O*-BQMAE (3) in  $CDCl_3$ ; Figure S13:  $^1H/^{13}C$  NMR spectrum of *N,N*-BQMAE (4) in  $CDCl_3$ ; Figure S14:  $^1H/^{13}C$  NMR spectrum of 6-MeO-*N,N*-BQMAE (5) in  $CDCl_3$ ; Figure S15:  $^1H/^{13}C$  NMR spectrum of TriMeO-*N,N*-BQMAE (6) in  $CDCl_3$ .

**Author Contributions:** Conceptualization, Y.M.; investigation, Y.M., A.T., H.K. (Hinata Koike), S.S., and H.K. (Hideo Konno); writing—original draft preparation, Y.M.; writing—review and editing, S.S.; supervision, Y.M.; project administration, Y.M.; funding acquisition, Y.M. All authors have read and agreed to the published version of the manuscript.

**Funding:** This research was funded by the Grant-in-Aid for Scientific Research provided by the JSPS KAKENHI Grant Number JP19H04583 and JP23K04808, and the Nara Women's University Intramural Grant for Project Research.

**Institutional Review Board Statement:** Not applicable.

**Informed Consent Statement:** Not applicable.

**Data Availability Statement:** Data are contained within the article and supplementary materials.

**Conflicts of Interest:** The authors declare no conflicts of interest.

## References

1. USGS (United States Geological Survey). *Mineral Commodity Summaries*; United States Geological Survey: Reston, VA, USA, 2018; pp. 40–41.
2. Agency for Toxic Substances and Disease Registry. 2022 Substance Priority List. Available online: <https://www.atsdr.cdc.gov/SPL/#2022spl> (accessed on 6 January 2024).
3. Taki, M. Imaging and Sensing of Cadmium in Cells. In *Metal Ions in Life Sciences*; Springer Science+Business Media: Dordrecht, The Netherlands, 2013; Volume 11, pp. 99–115.
4. Kim, H.N.; Ren, W.X.; Kim, J.S.; Yoon, J. Fluorescent and colorimetric sensors for detection of lead, cadmium, and mercury ions. *Chem. Soc. Rev.* **2012**, *41*, 3210–3244. [[CrossRef](#)] [[PubMed](#)]
5. Khairy, M.; El-Safty, S.A.; Shenashen, M.A. Environmental remediation and monitoring of cadmium. *Trends Anal. Chem.* **2014**, *62*, 56–68. [[CrossRef](#)]
6. Qian, X.; Xu, Z. Fluorescence imaging of metal ions implicated in diseases. *Chem. Soc. Rev.* **2015**, *44*, 4487–4493. [[CrossRef](#)] [[PubMed](#)]
7. Wu, D.; Sedgwick, A.C.; Gunnaugsson, T.; Akkaya, E.U.; Yoon, J.; James, T.D. Fluorescent chemosensors: The past, present and future. *Chem. Soc. Rev.* **2017**, *46*, 7105–7123. [[CrossRef](#)] [[PubMed](#)]
8. Wang, X.; Shen, C.; Zhou, C.; Bu, Y.; Yan, X. Methods, principles and applications of optical detection of metal ions. *Chem. Eng. J.* **2021**, *417*, 129125. [[CrossRef](#)]
9. Chen, S.-Y.; Li, Z.; Li, K.; Yu, X.-Q. Small molecular fluorescent probes for the detection of lead, cadmium and mercury ions. *Coord. Chem. Rev.* **2021**, *429*, 213691. [[CrossRef](#)]
10. AbhijnaKrishna, R.; Velmathi, S. A review on fluorimetric and colorimetric detection of metal ions by chemodosimetric approach 2013–2021. *Coord. Chem. Rev.* **2022**, *459*, 214401. [[CrossRef](#)]
11. Li, Z.; Hou, J.-T.; Wang, S.; Zhu, L.; He, X.; Shen, J. Recent advances of luminescent sensors for iron and copper: Platforms, mechanisms, and bio-applications. *Coord. Chem. Rev.* **2022**, *469*, 214695. [[CrossRef](#)]
12. Wang, J.; Meng, Q.; Yang, Y.; Zhong, S.; Zhang, R.; Fang, Y.; Gao, Y.; Cui, X. Schiff Base Aggregation-Induced Emission Luminogens for Sensing Applications: A Review. *ACS Sens.* **2022**, *7*, 2521–2536. [[CrossRef](#)]
13. Luo, D.; Huang, J.; Jian, Y.; Singh, A.; Kumar, A.; Liu, J.; Pan, Y.; Ouyang, Q. Metal-organic frameworks (MOFs) as apt luminescent probes for the detection of biochemical analytes. *J. Mater. Chem. B* **2023**, *11*, 6802–6822. [[CrossRef](#)]
14. Shi, C.; Li, X.; Liu, Q.; Kushwaha, A.; Prakash, O.; Sakiyama, H.; Muddassir, M.; Kumar, A.; Liu, J. Selective and sensitive sensing of copper(II) by natural compound C-21 steroid caudatin. *Polyhedron* **2023**, *243*, 116537. [[CrossRef](#)]

15. Tan, G.; Wang, S.; Yu, J.; Chen, J.; Liao, D.; Liu, M.; Nezamzadeh-Ejehieh, A.; Pan, Y.; Liu, J. Detection mechanism and the outlook of metal-organic frameworks for the detection of hazardous substances in milk. *Food Chem.* **2024**, *430*, 136934. [[CrossRef](#)] [[PubMed](#)]
16. Xue, L.; Liu, C.; Jiang, H. Highly Sensitive and Selective Fluorescent Sensor for Distinguishing Cadmium from Zinc Ions in Aqueous Media. *Org. Lett.* **2009**, *11*, 1655–1658. [[CrossRef](#)] [[PubMed](#)]
17. Xu, Z.; Baek, K.-H.; Kim, H.N.; Cui, J.; Qian, X.; Spring, D.R.; Shin, I.; Yoon, J. Zn<sup>2+</sup>-Triggered Amide Tautomerization Produces a Highly Zn<sup>2+</sup>-Selective, Cell-Permeable, and Ratiometric Fluorescent Sensor. *J. Am. Chem. Soc.* **2010**, *132*, 601–610. [[CrossRef](#)] [[PubMed](#)]
18. Lu, C.; Xu, Z.; Cui, J.; Zhang, R.; Qian, X. Ratiometric and Highly Selective Fluorescent Sensor for Cadmium under Physiological pH Range: A New Strategy to Discriminate Cadmium from Zinc. *J. Org. Chem.* **2007**, *72*, 3554–3557. [[CrossRef](#)] [[PubMed](#)]
19. Cai, Y.; Meng, X.; Wang, S.; Zhu, M.; Pan, Z.; Guo, Q. A quinoline based fluorescent probe that can distinguish zinc(II) from cadmium(II) in water. *Tetrahedron Lett.* **2013**, *54*, 1125–1128. [[CrossRef](#)]
20. Xue, L.; Liu, Q.; Jiang, H. Ratiometric Zn<sup>2+</sup> Fluorescent Sensor and New Approach for Sensing Cd<sup>2+</sup> by Ratiometric Displacement. *Org. Lett.* **2009**, *11*, 3454–3457. [[CrossRef](#)] [[PubMed](#)]
21. Mameli, M.; Aragoni, M.C.; Arca, M.; Caltagirone, C.; Demartin, F.; Farruggia, G.; De Filippo, G.; Devillanova, F.A.; Garau, A.; Isaia, F.; et al. A Selective, Nontoxic, OFF–ON Fluorescent Molecular Sensor Based on 8-Hydroxyquinoline for Probing Cd<sup>2+</sup> in Living Cells. *Chem. Eur. J.* **2010**, *16*, 919–930. [[CrossRef](#)]
22. Song, E.J.; Kang, J.; You, G.R.; Park, G.J.; Kim, Y.; Kim, S.-J.; Kim, C.; Harrison, R.G. A single molecule that acts as a fluorescence sensor for zinc and cadmium and a colorimetric sensor for cobalt. *Dalton Trans.* **2013**, *42*, 15514–15520. [[CrossRef](#)]
23. Xue, L.; Li, G.; Liu, Q.; Wang, H.; Liu, C.; Ding, X.; He, S.; Jiang, H. Ratiometric Fluorescent Sensor Based on Inhibition of Resonance for Detection of Cadmium in Aqueous Solution and Living Cells. *Inorg. Chem.* **2011**, *50*, 3680–3690. [[CrossRef](#)]
24. Zhang, Y.; Guo, X.; Zheng, M.; Yang, R.; Yang, H.; Jia, L.; Yang, M. A 4,5-quinolimide-based fluorescent sensor for the turn-on detection of Cd<sup>2+</sup> with live-cell imaging. *Org. Biomol. Chem.* **2017**, *15*, 2211–2216. [[CrossRef](#)] [[PubMed](#)]
25. Udhayakumari, D. A comprehensive anthology of literature based on quinoline chemosensors from 2006 to 2022. *J. Mol. Struct.* **2023**, *1287*, 135715. [[CrossRef](#)]
26. Mikata, Y. Quinoline- and isoquinoline-derived ligand design on TQEN (*N,N,N',N'*-tetrakis(2-quinolylmethyl)ethylenediamine) platform for fluorescent sensing of specific metal ions and phosphate species. *Dalton Trans.* **2020**, *49*, 17494–17504. [[CrossRef](#)] [[PubMed](#)]
27. Mikata, Y.; Kizu, A.; Nozaki, K.; Konno, H.; Ono, H.; Mizutani, S.; Sato, S. TQOPEN (*N,N,N',N'*-Tetrakis(2-quinolylmethyl)-3-oxa-1,5-pentanediamine) Family as Heptadentate Fluorescent Cd<sup>2+</sup> Sensors. *Inorg. Chem.* **2017**, *56*, 7404–7415. [[CrossRef](#)] [[PubMed](#)]
28. Mikata, Y.; Kaneda, M.; Konno, H.; Matsumoto, A.; Sato, S.; Kawamura, M.; Iwatsuki, S. Methoxy-substituted tetrakisquinoline analogs of EGTA and BAPTA for fluorescence detection of Cd<sup>2+</sup>. *Dalton Trans.* **2019**, *48*, 3840–3852. [[CrossRef](#)]
29. Mikata, Y.; Tanaka, M.; Yasuda, S.; Tsuruta, A.; Hagiwara, T.; Konno, H.; Matsuo, T. Effect of methoxy substituents on fluorescent Zn<sup>2+</sup>/Cd<sup>2+</sup> selectivity of bisquinoline derivatives with a *N,N'*-dimethylalkanediamine skeleton. *Dalton Trans.* **2023**, *52*, 7411–7420. [[CrossRef](#)]
30. Lu, H.-L.; Wang, W.-K.; Tan, X.-X.; Luo, X.-F.; Zhang, M.-L.; Zhang, M.; Zang, S.-Q. A new quinoline-based fluorescent probe for Cd<sup>2+</sup> and Hg<sup>2+</sup> with an opposite response in a 100% aqueous environment and live cell imaging. *Dalton Trans.* **2016**, *45*, 8174–8181. [[CrossRef](#)]
31. dos Santos Carlos, F.; da Silva, L.A.; Zanlorenzi, C.; Nunes, F.S. A novel macrocycle acridine-based fluorescent chemosensor for selective T detection of Cd<sup>2+</sup> in Brazilian sugarcane spirit and tobacco cigarette smoke extract. *Inorg. Chim. Acta* **2020**, *508*, 119634. [[CrossRef](#)]

**Disclaimer/Publisher's Note:** The statements, opinions and data contained in all publications are solely those of the individual author(s) and contributor(s) and not of MDPI and/or the editor(s). MDPI and/or the editor(s) disclaim responsibility for any injury to people or property resulting from any ideas, methods, instructions or products referred to in the content.